A Fast Wavelet-Based Algorithm for Global and Local Image Sharpness Estimation

Phong V. Vu and Damon M. Chandler

***Abstract*— In this paper, we present a simple, yet effective wavelet-based algorithm for estimating both global and local image sharpness (FISH, *F*ast *I*mage *Sh*arpness). FISH operates by first decomposing the input image via a three-level separable discrete wavelet transform (DWT). Next, the log-energies of the DWT subbands are computed. Finally, a scalar index corresponding to the image's overall sharpness is computed via a weighted average of these log-energies. Testing on several image databases demonstrates that, despite its simplicity, FISH is competitive with the currently best-performing techniques both for sharpness estimation and for no-reference image quality assessment.**

I. INTRODUCTION

A useful goal in image processing is to determine whether one image (region) appears sharper than another. Algorithms which can automatically predict perceived sharpness or blurriness are known as *sharpness estimators* or *blurriness estimators*, respectively. Such algorithms have been shown to be useful for tasks such as main-subject detection, image quality assessment, and image restoration (see [1] for relevant references).

Previous methods of sharpness/blurriness estimation have employed a wide variety of approaches [2]–[6]. The vast majority of these methods operate under the assumption that the appearance of edges is affected by blur, and accordingly these methods estimate sharpness/blurriness by using various edge-appearance models. For example, Ferzli *et al.* [3] measure edge widths in 8×8 blocks, which are then weighted by a Mean Just-Noticeable Blur factor (see also [4]). Liu *et al.* [5] employ edge features extracted by using a Sobel edge detector, and then combine these features via a circular back-propagation neural network system for blur estimation. Li *et al.* [6] compare the kurtoses of blocks of dominant edge pixels in the input image with those of a purposely re-blurred version.

Other methods have used spectral information to estimate sharpness [7]–[9]. For example, Shaked *et al.* [7] use the DFT to estimate sharpness based on the ratio of high-pass to low-pass energy of the the spatial derivative of each line/column. Sharpness has also been estimated based on the peakedness of the energy spectrum [8], and on the uniformity of the energy spectrum [9].

Phong V. Vu and Damon M. Chandler, 202 Engineering South, School of Electrical and Computer Engineering, Oklahoma State University, Stillwater, OK 74078 USA. Email: phong.vu, damon.chandler@okstate.edu, Telephone: (405) 744–9924, Fax: (405) 744–9198.

This project was supported by the National Science Foundation, Grant Number 1054612.

Various DCT, DWT, and other transforms have also been used either to detect edges and/or to model edge-appearance. Sharpness/blurriness has been estimated based on the kurtosis of DWT coefficients corresponding to edge blocks [10], based on the Lipschitz exponent of the sharpest edges [11], based on edge types [12], and based on local phase coherence measured via complex wavelets [13].

More recently, hybrid approaches have been developed which employ a combination of edge-/pixel-based and transform-based methods [14], [1]. For example, Chen *et al.* [14] proposed a blur metric that employs the statistics of the image gradient histogram and a wavelet-based detail map. Vu *et al.* [1] used a block-based approach to develop the first method specifically designed to measure local sharpness. Their method estimates the spatial and spectral sharpness of local image regions using the slope of the local magnitude spectrum and the local total variation; these values are then combined to generate an image sharpness map. Hybrid approaches have generally proven to perform better than edge-only-based or transform-only-based methods, though at the expense of added computational complexity.

In this paper, we present a sharpness estimator, called *FISH* (*F*ast *I*mage *Sh*arpness), which offers the simplicity of a spectral-based method but with the improved predictive performance of a hybrid method. Following from [7] and [8], FISH operates under the assumption that perceived sharpness can be estimated by examining the energy in high-frequency bands. Here, we use a three-level separable discrete wavelet transform (DWT) and measure the log-energy of the DWT subbands. Sharpness is estimated based on a weighted geometric mean of these log-energies. As we will demonstrate, despite its simplicity, FISH is competitive with the currently best-performing techniques. In addition, by clustering DWT coefficients, we show how FISH can be easily modified to yield a map indicating the relative sharpness of each image region. Thus, unlike most existing methods (with the exception of [1]), FISH can generate sharpness maps.

This paper is organized as follows: In Section II, we provide details of the FISH algorithm. Section III presents results of FISH on within-image and across-image sharpness estimation, and on no-reference quality assessment of blurred images; this section also includes a discussion of runtime requirements. General conclusions are presented in Section IV.

II. ALGORITHM

A. Global Image-Based FISH

Given a grayscale input image I, the FISH algorithm consists of the following three steps:

1) Step 1: Compute the DWT: The grayscale input image is decomposed into wavelet subbands by using the Cohen-Daubechies-Fauraue 9/7 filters [15] with three levels of decomposition. Let S_{LH_n}, S_{HL_n}, S_{HH_n} denote the LH, HL, and HH subbands at DWT level $n \in [1, 3]$. (The LL_3 subband is not used.)

2) Step 2: Compute the Log-Energy at each DWT Level: Images which appear sharp generally contain more high-frequency content than images which appear smooth/blurred. To quantify this effect, we first measure the log-energy of each subband at each decomposition level as follows:

$$E_{XY_n} = \log_{10}(1 + \frac{1}{N_n} \sum_{i,j} S^2_{XY_n}(i,j)), \tag{1}$$

where XY is either LH, HL or HH. The quantity N_n is the number of DWT coefficients in the subband at level n. The addition of one is used to prevent negative values of E_{XY_n}.

Next, we measure the total log-energy at each decomposition level via

$$E_n = (1 - \alpha)\frac{E_{LH_n} + E_{HL_n}}{2} + \alpha E_{HH_n}, \tag{2}$$

where the parameter $\alpha = 0.8$ was chosen empirically to give greater weight to the energy in the HH subband; this band can be regarded to span a higher radial spatial frequency (by a factor of $\sqrt{2}$) than the LH and HL bands.

3) Step 3: Compute the Sharpness Index: Finally, the three per-level log-energy values E_1, E_2, and E_3 are combined as follows to determine a scalar sharpness index representing the image's overall sharpness:

$$\text{FISH} = \sum_{n=1}^{3} 2^{3-n} E_n. \tag{3}$$

Here, FISH ≥ 0, is the overall sharpness index; the larger the index, the greater the perceived sharpness. The factor $2^{3-n} = \{4, 2, 1\}$ when $n = \{1, 2, 3\}$ is used to provide greater weight to the finer scales (higher-frequency bands).

B. Local Block-Based FISH

The previous section described the FISH algorithm applied to the entire image. It is also possible to apply the algorithm in a block-based fashion to determine a map denoting local perceived sharpness.

To generate the sharpness map, we compute a collection of local FISH values using the DWT coefficients corresponding to each 16×16 block of the image. Following the procedure described in [16], each subband is divided into small blocks of size 8×8, 4×4, and 2×2 for levels 1, 2, and 3, respectively. As shown in Figure 1, the 16×16 DWT coefficients corresponding to the top-left 16×16 block of the image are assembled by taking three 8×8 blocks from the level-1 bands, three 4×4 blocks from the level-2 bands, and three 2×2 blocks from the level-3 bands. Equation (3) is then applied to these 16×16 coefficients to compute a FISH index for this top-left block.

This process is repeated for each 16×16 block with 50% overlap between two consecutive blocks of DWT coefficients to generate a sharpness map. Because we use 50% of overlap between neighboring blocks, each pixel in the sharpness map corresponds to a block size of 8×8 in the input image. Figure 1 (*right*), illustrates the sharpness map of the image *lena*.

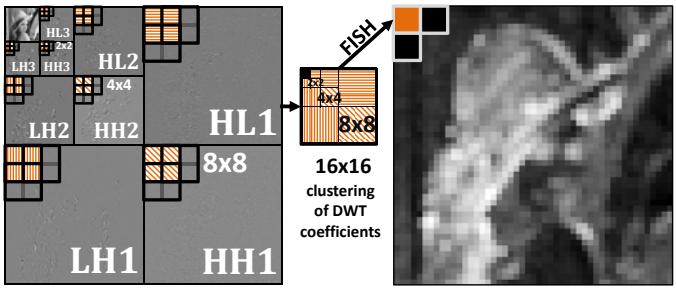

Fig. 1. Illustration of DWT coefficients clustering into a 16x16 wavelet block with 50% overlap to generate the sharpness map. *The orange pixel and its two adjacent pixels in the sharpness map are shown according to the orange striped set of DWT coefficients and two adjacent sets of DWT coefficients with 50% overlap.* Note that, to promote visibility, the size of the blocks and sharpness map are not drawn to scale; the map is 64×64 pixels for a 512×512 input image.

It is also possible to collapse the sharpness map into a scalar sharpness index representing the image's overall sharpness. This index, FISH$_{bb}$, is computed by taking the root mean square of the 1% largest values of the local sharpness (FISH) indices (following from [1]):

$$\text{FISH}_{bb} = \sqrt{\frac{1}{T}\sum_{i=1}^{T} \text{FISH}_i^2}, \tag{4}$$

where T denotes the number of blocks which received the 1% largest FISH indices of the sharpness map; and where FISH$_i$, $i = 1, 2, .., T$ denotes the FISH indices of these blocks. The value of 1% is used because, as argued in [1], the overall perceived sharpness of an image is largely determined by the image's sharpest regions.

III. Results and Discussion

A. Representative Results

Figure 2 shows representative results that demonstrate the ability of FISH/FISH$_{bb}$ to accurately estimate across-image and within-image sharpness (FISH$_{bb}$ only) for a variety of images containing different sharpness levels. The images are ordered based on subjective ratings of sharpness [1].

In terms of across-image sharpness, the FISH/FISH$_{bb}$ indices generally match the relative perceived sharpness across these images. For example, two of the images, *petal* and *zebra*, are not as sharp as images *pelicans* and *branches*, but are clearly much sharper than image *ball*. Both FISH and FISH$_{bb}$ fail to predict the sharpness of image *petal* in comparison to either image *airplane* (for FISH) or image *zebra* (for FISH$_{bb}$). We believe that these failure cases are attributable to the fact that neither FISH nor FISH$_{bb}$ take into account local contrast. Such a measurement could be implemented, though at the expense of added complexity.

In terms of within-image sharpness, FISH$_{bb}$ correctly estimates the perceived sharpness of each image region. For

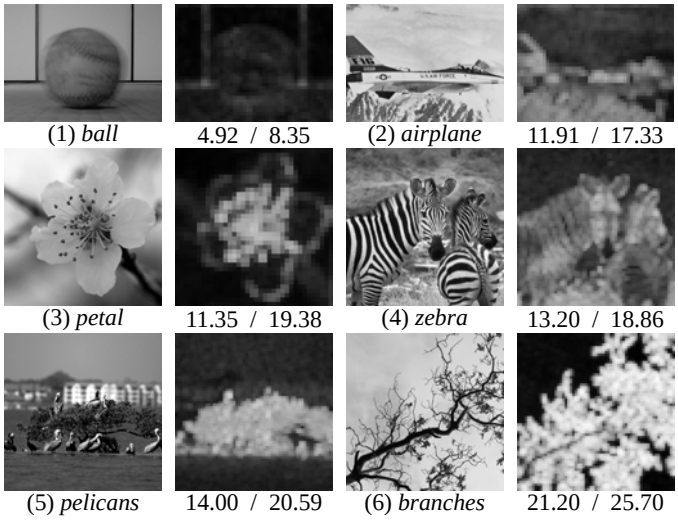

Fig. 2. Representative maps generated by using $FISH_{bb}$ along with sharpness indices computed via FISH/$FISH_{bb}$. The images were selected and organized in the order of overall sharpness judged by human subjects [1].

example, in image *petal*, the flower's stamens and the edges of the petals are the sharpest regions in this image; these regions are accurately highlighted in the corresponding $FISH_{bb}$ map. Similarly, in image *branches*, the branches are much sharper than the sky; this fact is reflected in the $FISH_{bb}$ map.

B. No-Reference Quality Assessment of Blurred Images

To evaluate the performance of FISH on no-reference quality assessment of blurred images, we used the blurred image subsets from four image-quality databases: (1) The LIVE database [17] (containing 145 blurred images); (2) the IVC database [18] (20 blurred images); (3) the TID database [19] (96 blurred images); and (4) the CSIQ database [20] (150 blurred images). We compared our method against five sharpness estimators (ST [7], JNBM [3], CPBD [4], LPCM [13], and S_3 [1]), two blurriness estimators (MMZ [21] and MDWE [2]), and one no-reference image quality estimator (BLIINDS-II [22]), for which code is publicly available. The performance of predicting subjective ratings of quality was measured in terms of the Spearman rank-order correlation coefficient (SROCC) for gauging prediction monotonicity; the Pearson linear correlation coefficient (CC) (following non-linear regression; see [1]) for gauging prediction consistency; and the outlier ratio (OR) and outlier distance (OD) [20] for outlier analysis.

Table I shows the results of this evaluation. Both FISH and $FISH_{bb}$ perform quite well on all four databases. In terms of CC and SROCC, $FISH_{bb}$ outperforms other methods on the two largest databases (CSIQ and LIVE2) and is competitive on the other two databases; FISH and MMZ are the two best methods on IVC. In terms of outliers, $FISH_{bb}$ also shows the best performance. Note that BLIINDS-II is a general quality estimator, and not a sharpness/blurriness estimator; its performance here is thus noteworthy.

TABLE I
PERFORMANCES OF VARIOUS ALGORITHMS ON NO-REFERENCE QUALITY ASSESSMENT OF BLURRED IMAGES; THE TWO BEST RESULTS ARE HIGHLIGHTED; THE LAST COLUMN SHOWS THE AVERAGE WEIGHTED BY NUMBER OF IMAGES IN EACH DATABASE.

	LIVE2	IVC	TID	CSIQ	Avg.
	SROCC				
JNBM	0.787	0.666	0.714	0.762	0.755
CPBD	0.919	0.769	**0.854**	0.885	0.884
ST	0.702	0.406	0.516	0.705	0.645
MMZ	0.860	**0.971**	0.732	0.860	0.835
MDWE	0.804	0.685	0.717	0.770	0.765
BLIINDS-II	0.911	0.593	**0.872**	0.883	0.876
LPCM	0.928	0.835	0.803	0.905	0.886
S_3	**0.944**	0.869	0.850	**0.906**	**0.904**
FISH	0.881	**0.932**	0.786	0.894	0.866
$FISH_{bb}$	**0.938**	0.919	0.841	**0.917**	**0.907**
	CC				
JNBM	0.816	0.698	0.727	0.806	0.786
CPBD	0.895	0.801	0.848	0.882	0.875
ST	0.704	0.603	0.621	0.690	0.674
MMZ	0.885	**0.956**	0.753	0.889	0.859
MDWE	0.806	0.711	0.709	0.797	0.775
BLIINDS-II	0.912	0.800	***0.859***	0.908	0.893
LPCM	0.917	0.949	0.811	0.911	0.892
S_3	**0.943**	0.928	**0.877**	0.911	**0.914**
FISH	0.904	**0.957**	0.816	**0.923**	0.893
$FISH_{bb}$	**0.944**	0.941	***0.858***	**0.943**	**0.923**

	LIVE2	CSIQ		LIVE2	CSIQ
	OR			**OD**	
JNBM	68.97%	36.67%	JNBM	710.328	6.282
CPBD	62.76%	37.33%	CPBD	441.704	4.269
ST	76.55%	42.67%	ST	956.765	10.368
MMZ	66.90%	31.33%	MMZ	529.762	3.674
MDWE	64.83%	34.00%	MDWE	703.935	6.380
BLIINDS-II	64.83%	***26.00%***	BLIINDS-II	418.430	3.111
LPCM	58.62%	31.33%	LPCM	411.010	3.093
S_3	**53.10%**	32.67%	S_3	**285.968**	3.031
FISH	64.83%	***26.00%***	FISH	470.833	**2.417**
$FISH_{bb}$	**54.48%**	**24.00%**	$FISH_{bb}$	**289.850**	**1.648**

TABLE II
LOCAL SHARPNESS PREDICTION ACCURACY

	S_3	$FISH_{bb}$	S_3	$FISH_{bb}$	S_3	$FISH_{bb}$
Image	**SROCC**		**CC**		**RMSE**	
dragon	**0.931**	0.923	0.947	**0.950**	26.414	**26.016**
flower	0.712	**0.749**	**0.936**	0.927	**28.805**	31.191
monkey	**0.916**	0.897	0.944	**0.959**	29.801	**25.906**
orchid	**0.920**	0.910	0.914	**0.929**	39.671	**36.221**
peak	0.901	**0.912**	**0.928**	0.927	**29.461**	29.662
squirrel	0.794	**0.854**	**0.958**	0.954	**29.683**	31.256
Average	0.862	**0.874**	0.938	**0.941**	30.639	**30.042**

C. Local Sharpness Estimation

We compared the sharpness maps from $FISH_{bb}$ with ground-truth sharpness maps obtained from human subjects [1]. Figure 3 shows three original images and the corresponding sharpness maps obtained from human subjects and estimated by S_3 and $FISH_{bb}$. The S_3 algorithm was specifically designed to generate sharpness maps and was shown in [1] to generally yield the best map predictions. As shown in Figure 3, $FISH_{bb}$ can yield maps which are quite competitive with S_3's maps. This latter assertion is quantified in Table II, which shows the SROCC, CC (after non-linear regression), and RMSE between the ground-truth sharpness maps and the maps predicted via S_3 and $FISH_{bb}$.

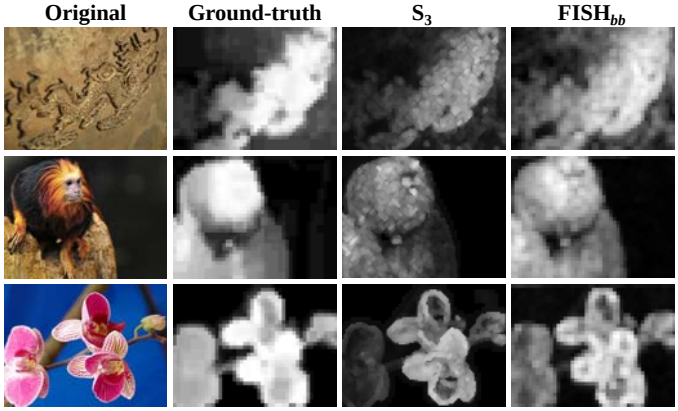

Fig. 3. Local sharpness maps of three images *dragon, monkey, orchid* generated by human subjects, S_3 [1], and $FISH_{bb}$.

TABLE III
RUNTIME REQUIREMENTS (SECONDS/IMAGE); THE TWO FASTEST METHODS ARE HIGHLIGHTED.

	512×512	1024×768	1280×960	1600×1200
JNBM	1.854	5.563	8.779	14.812
CPBD	2.162	7.364	12.306	22.927
ST	**0.210**	**1.041**	**1.991**	**4.086**
MMZ	0.608	1.859	2.985	5.024
MDWE	0.914	3.712	7.225	14.273
BLIINDS-II	145.189	443.860	696.720	1176.00
LPCM	0.909	2.852	4.151	6.688
S_3	29.154	64.522	122.640	142.841
FISH	**0.079**	**0.259**	**0.469**	**0.611**
$FISH_{bb}$	1.309	4.018	6.291	10.126

D. Runtime vs. Image Size

To evaluate runtime, we applied FISH, $FISH_{bb}$, and the other estimators to images of size 512×512, 1024×768, 1280×960, and 1600×1200 pixels. Table III shows the average runtime of each algorithm in seconds, where the average was taken over 100 trials. This test was performed using a modern desktop computer (Intel Quad Core at 2.66 GHz, 12 GB RAM DDR2 at 6400 MHz, Windows 7 Pro 64-bit, Matlab 7.8). All of the methods were implemented in Matlab.

As shown in Table III, FISH is the fastest algorithm for all image sizes, and $FISH_{bb}$ is still significantly faster than the methods which yield competitive predictive performance (S_3, JNBM, CPBD, and BLIINDS-II; see Table I). In terms of memory requirements, both FISH and $FISH_{bb}$ have the same memory requirements as a standard DWT with only a negligible amount of additional memory needed for the output map (for $FISH_{bb}$) and other scalar variables.

IV. CONCLUSIONS

This paper presented a simple, yet effective algorithm (FISH) for estimating both global and local image sharpness. FISH operates by first decomposing the input image via a three-level separable DWT, and then estimating sharpness based on a weighted geometric mean of the DWT subband energies. To generate a local sharpness map, FISH can be operated in a block-based fashion ($FISH_{bb}$) by applying the same computation to groups of DWT coefficients. We demonstrated the efficacy of FISH/$FISH_{bb}$ on several image databases.

REFERENCES

[1] C.T. Vu, T.D. Phan, and D.M. Chandler, "S_3: A spectral and spatial measure of local perceived sharpness in natural images," *IEEE Transactions on Image Processing*, vol. 21, no. 3, Mar 2012.

[2] P. Marziliano, F. Dufaux, S. Winkler, and T. Ebrahimi, "A no-reference perceptual blur metric," *IEEE International Conference on Image Processing, 2002. ICIP 2002.*, vol. 3, 2002.

[3] R. Ferzli and L.J. Karam, "A no-reference objective image sharpness metric based on the notion of just noticeable blur (JNB)," *IEEE Transactions on Image Processing*, vol. 18, no. 4, Apr 2009.

[4] N.D. Narvekar and L.J. Karam, "A no-reference perceptual image sharpness metric based on a cumulative probability of blur detection," *International Workshop on Quality of Multimedia Experience, QoMEx*, Jul 2009.

[5] H. Liu, J. Wang, J. Redi, P. Le Callet, and I. Heynderickx, "An efficient no-reference metric for perceived blur," *European Workshop on Visual Information Processing, 2011. EUVIP 2011.*, Jul 2011.

[6] C. Li, W. Yuan, A.C. Bovik, and X. Wu, "No-reference blur index using blur comparisons," *IEEE Electronics Letters*, vol. 47, no. 17, 2011.

[7] D. Shaked and I. Tastl, "Sharpness measure: towards automatic image enhancement," *IEEE International Conference on Image Processing, 2005. ICIP 2005.*, vol. 1, Sep 2005.

[8] N. Zhang, A. E. Vladar, M. T. Postek, and B. Larrabee, "A kurtosis-based statistical measure for two-dimensional processes and its application to image sharpness," *Section of Physical and Engineering Sciences of American Statistical Society*, 2003.

[9] M. Kristan, J. Per, M. Pere, and S. Kovacic, "A bayes-spectral-entropy-based measure of camera focus using a discrete cosine transform," *Pattern Recognition Letters*, vol. 27, no. 13, 2006.

[10] R. Ferzli, L.J. Karam, and J. Caviedes, "A robust image sharpness metric based on kurtosis measurement of wavelet coefficients," *International Workshop on Video Processing and Quality Metrics for Consumer Electronics*, Jan 2005.

[11] F. Rooms, A. Pizurica, and W. Philips, "Estimating image blur in the wavelet domain," *IEEE International Conference on Acoustics, Speech, and Signal Processing, 2002. ICASSP 2002.*, vol. 4, May 2002.

[12] H. Tong, M. Li, H. Zhang, and C. Zhang, "Blur detection for digital images using wavelet transform," *IEEE International Conference on Multimedia and Expo, 2004. ICME 2004.*, vol. 1, Jun 2004.

[13] R. Hassen, Z. Wang, and M. Salama, "No-reference image sharpness assessment based on local phase coherence measurement," *IEEE International Conference on Acoustics Speech and Signal Processing, 2010. ICASSP 2010.*, Mar 2010.

[14] M.J. Chen and A.C. Bovik, "No-reference image blur assessment using multiscale gradient," *International Workshop on Quality of Multimedia Experience, QoMEx*, Jul 2009.

[15] A. Cohen, I. Daubechies, and J.-C. Feauveau, "Biorthogonal bases of compactly supported wavelets," *Communications on Pure and Applied Mathematics*, vol. 45, Jun 1992.

[16] H.W. Park and H.S. Kim, "Motion estimation using low-band-shift method for wavelet-based moving-picture coding," *IEEE Transactions on Image Processing*, vol. 9, no. 4, Apr 2000.

[17] H.R. Sheikh, Z. Wang, L. Cormack, and A.C. Bovik, "Live image quality assessment database release 2," Available: http://live.ece.utexas.edu/research/quality.

[18] A. Ninassi, P.L. Callet, and F. Autrusseau, "Pseudo no reference image quality metric using perceptual data hiding," *Proc. SPIE Human Vision and Electronic Imaging XI*, vol. 6057, Feb 2006.

[19] N. Ponomarenko, V. Lukin, A. Zelensky, K. Egiazarian, J. Astola, M. Carli, and F. Battisti, "TID2008 - A database for evaluation of full-reference visual quality assessment metrics," *Advances of Modern Radioelectronics*, vol. 10, 2009.

[20] E.C. Larson and D.M. Chandler, "Most apparent distortion: Full-reference image quality assessment and the role of strategy," *Journal of Electronic Imaging*, vol. 19, no. 1, pp. 011006, 2010.

[21] X. Marichal, W.Y. Ma, and H.J. Zhang, "Blur determination in the compressed domain using DCT information," *IEEE International Conference on Image Processing, 1999. ICIP 1991.*, vol. 2, 1999.

[22] M.A. Saad, A.C. Bovik, and C. Charrier, "Model-based blind image quality assessment using natural DCT statistics," *IEEE Transactions on Image Processing*, appear 2011.